

## Spectroscopic and Thermal Characterization of the Swelling Behavior of Nafion Membranes in Mixtures of Water and Methanol

A. Martinez-Felipe,<sup>1</sup> C. T. Imrie,<sup>2</sup> A. Ribes-Greus<sup>1</sup>

<sup>1</sup>Institute of Materials Technology, Universitat Politècnica de València, Camino de Vera s/n, 46022, Valencia, Spain

<sup>2</sup>Department of Chemistry, School of Natural and Computing Sciences, Meston Building, University of Aberdeen, Aberdeen, AB24 3UE, Scotland, United Kingdom

Correspondence to: A. Ribes-Greus (E-mail: aribes@ter.upv.es)

**ABSTRACT:** The spectroscopic and thermal properties of swollen Nafion membranes in methanol aqueous mixtures were investigated to understand the behavior of commercial electrolytes in the presence of polar solvents. Several differences were observed in the absorption processes depending on the composition of the solvent. Deconvolution methods were applied to study specific contributions of solvents and polymer groups based on Fourier transform infrared spectroscopy and thermogravimetric analysis. The results evidence compositional effects on the interactions between solvents and Nafion. A major influence of the nonpolar domains (hydrophobic regions) in the absorption of methanol together with a reduction of the interactions with sulfonate groups was observed. Such changes are accompanied by a modification of the cluster morphology of the equilibrated membranes evaluated by differential scanning calorimetry. These findings can be useful to improve the knowledge on Nafion's microstructure in the presence of polar solvents. © 2012 Wiley Periodicals, Inc. *J. Appl. Polym. Sci.* 000: 000–000, 2012

**KEYWORDS:** thermal properties; infrared spectroscopy; membranes

Received 2 August 2011; accepted 11 April 2012; published online

**DOI:** 10.1002/app.37881

### INTRODUCTION

Nafion is probably the most common ionomeric material, manufactured by DuPont, and has been widely applied as perm-selective membrane separator in electrochemical cells, in Donnan dialysis cells, ionic polymeric transducers, water electrolyzers, electrochromic devices, sensors, or as strong acid catalysts.<sup>1</sup> It is also the benchmark electrolyte in low temperature fuel cells fed by hydrogen<sup>2–5</sup> and has also been used in direct methanol and ethanol fuel cells (DMFC and DEFC, respectively).<sup>1,2,6–12</sup> Its chemical structure consists of a perfluorinated backbone polytetrafluoroethylene (PTFE) and perfluoroalkyl ether side chains (PFAE) containing pendant SO<sub>3</sub>X residues (where X denotes an alkaline metal, such as sodium, potassium or lithium, or hydrogen). The perfluorinated chains form the hydrophobic domains and provide the material with high mechanical and chemical stability, while the ionic groups act as hydrophilic sites for the absorption of polar solvents and proton exchange.<sup>1,2,6–12</sup> As most ionomers, Nafion presents a complex supramolecular structure based on ionic aggregation and hydrophilic/hydrophobic microphase separation. When solvents are absorbed in the polymer, the balance between the hydrophilic

and hydrophobic regions is altered due to additional intermolecular interactions. Understanding the resulting morphology under working conditions is crucial to describe and improve the performance of Nafion and its derivatives.<sup>7–12</sup>

A number of models have been proposed attempting to describe the morphology of Nafion and the effect of absorption of polar solvents (see, for example, Refs. 13–22). Although these models vary in their detail, in essence each suggests that the microstructure of Nafion consists of a network of interconnected ionic aggregates or clusters in the perfluorinated polymer matrix, agreeing with Eisenberg's classical model for ionomers.<sup>23</sup> Within this broad framework, the absorption and transport of vapor and liquid water in Nafion has been studied extensively, and it is widely assumed that water (as well as other polar solvents) is absorbed through the ionic regions or phases by filling the ionic clusters, forming a network of pools and channels which enhance proton conductivity.<sup>14,24,25</sup> The details of this mechanism vary slightly depending on differences in the proposed morphology, particularly relating to interphase effects and specific experimental conditions.<sup>1,26</sup> When Nafion is swollen in organic solvents, the mechanisms associated with absorption may

change due the different polarity of the solvent molecules.<sup>27</sup> Several studies indicate the presence of methanol in both the hydrophilic and hydrophobic domains and in interphase regions of the polymer. When binary mixtures of solvents are absorbed, the mechanisms are even more complex due to the existence of interactions between the different solvent molecules.<sup>28</sup>

In this article, several commercial Nafion membranes in the H-acid form have been submitted to swelling tests in water, methanol and water-methanol binary mixtures to better understand such polymer/solvent interactions which may determine the resulting sorption behavior. The swollen membranes were characterised using Fourier transform infrared spectroscopy (FTIR) to investigate the short-range interactions of the polar and non-polar groups of the polymer with the solvents.<sup>29</sup> Thermogravimetric analysis (TGA) was used to establish the thermal stability of the swollen membranes and the solvent state whereas differential scanning calorimetry (DSC) provided information on the phase behavior.<sup>30</sup>

## EXPERIMENTAL PROCEDURE

Nafion membranes in the H-form with equivalent weight EW = 1100 were purchased from Fuel Cell Scientific, were stored in a dry environment and used as received. The water-methanol binary mixtures were prepared using 99.9% methanol (purchased from Sigma-Aldrich) and distilled water. The thicknesses of the membranes were measured using a clock Comparator Stand (Mitutoyo) to  $\pm 1 \mu\text{m}$  accuracy. The thickness was calculated as the mean of triplicate measurements made across different parts of the membranes, providing an average value of  $\varepsilon = 161 \mu\text{m} \pm 1 \mu\text{m}$ .

### Swelling Tests

The commercial membranes were cut into rectangular films measuring  $4 \times 1 \text{ cm}^2$ , weighed and placed in test tubes containing binary solutions of water and methanol. The compositions of the binary solutions were 10, 20, 30, and 40% by weight percentage of methanol, corresponding to methanol molar fractions of 0.06, 0.12, 0.19, and 0.27, respectively. Control samples were also placed in tubes containing pure water and pure methanol. The swelling experiments were performed in a thermostatic SELECTA Ultrasonic bath (accuracy  $0.1^\circ\text{C}$ ) at  $35^\circ\text{C}$ , to simulate the operating temperature of the electrolytes in a typical DMFC.

The absorption of solvent was measured gravimetrically several times during the swelling experiment, until constant weight was reached. The samples were removed from the test tubes and the excess liquid was removed using a tissue, weighed using a Mettler Toledo balance, and subsequently placed back into the test tubes in the isothermal bath. Following the last measurement, the samples were covered and stored for further analysis. All the experiments described were performed three times using different membranes to obtain average values. The samples are referred as MeOH-*X*, where *X* is the weight percentage of methanol in the solution in which they were immersed. The unswollen Nafion membrane is simply referred as Nafion (see Table I).

**Table I.** Parameters of the Swelling Tests Performed in Binary Mixtures of Water and Methanol; for Definitions See Text

Sample	$S_{\text{eq}}$ (%)	$t_{1/2}$ (min)
MeOH-0	18.3	10.7
MeOH-10	24.3	11.9
MeOH-20	32.9	12.6
MeOH-30	39.5	12.8
MeOH-40	50.9	17.6
MeOH-100	122.1	18.2

### Attenuated Total Reflectance—Fourier Transform Infrared Spectroscopy (ATR-FTIR)

The FTIR experiments were performed using a Thermo Nicolet 5700 spectrometer (MA, Waltham) equipped with an ATR accessory. Samples were placed on a diamond crystal, and the experiments were performed using 1 bounce and an incident angle of  $45^\circ\text{C}$ . The spectra were collected over 32 scans with an accuracy of  $4 \text{ cm}^{-1}$ . Background spectra were collected before each series of experiments. All the experiments were performed seven times and the average curves were calculated using the OMNIC software (Thermo-Scientific).

### Thermogravimetric Analysis

TGA experiments were performed using a Mettler Toledo TGA/SDTA 851 analyser (OH, Columbus). The experiments used a dynamic program from 25 to  $750^\circ\text{C}$  at a heating rate of 10 K/min under inert Argon (Ar) atmosphere with a flow rate of 200 mL/min. Sample masses were around 5 mg.

### Differential Scanning Calorimetry

The DSC thermograms were obtained using a Mettler Toledo DSC 822 analyser (OH, Columbus). The samples containing around 5 mg were heated from  $-50$  to  $200^\circ\text{C}$ , held at  $200^\circ\text{C}$  for 3 mins, cooled to  $-50^\circ\text{C}$ , held for 3 mins, and reheated to  $200^\circ\text{C}$ . All the scans were performed at  $10^\circ\text{C}/\text{min}$  under nitrogen atmosphere and using liquid nitrogen as the coolant.

## RESULTS AND DISCUSSION

### Swelling tests

The amount of solvent absorbed by a membrane during the swelling test was calculated as the difference between the mass of the sample immersed in the solutions for time  $t$  ( $w_t \pm 0.01 \text{ mg}$ ) and the unswollen sample ( $w_0 \pm 0.01 \text{ mg}$ ). The results were normalised with respect to the mass of the unswollen sample and expressed as a swelling percentage according to  $S_w(\%) = \frac{w_t - w_0}{w_0} \cdot 100$ . The swelling curves of the membranes immersed in water, methanol and water-methanol binary mixtures at  $35^\circ\text{C}$  showed a rapid absorption, during the first moments of the swelling experiments before the equilibrium is attained. The percentage of solvent absorbed at equilibrium,  $S_{\text{eq}} = S_w(t \rightarrow \infty)$ , and the time to reach half of the equilibrium swelling value,  $t_{1/2}$ , were obtained from the experimental swelling curves, and are listed in Table I. It is clear that Nafion membranes absorb considerably more methanol than water when immersed in the pure solvents. Also,  $S_{\text{eq}}$  increases on increasing methanol concentration in the mixtures. These observations are in good agreement with previous studies.<sup>31–33</sup>

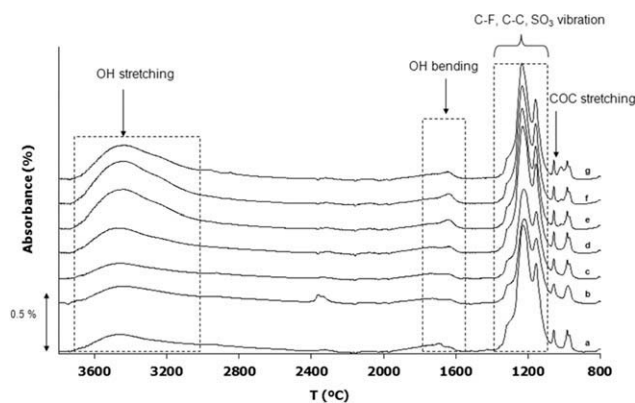


**Figure 1.** FTIR-ATR spectra of the Nafion membranes immersed in water, methanol and water-methanol mixtures at 35°C: (a) Unswollen Nafion, (b) MeOH-0 (water), (c) MeOH-10, (d) MeOH-20, (e) MeOH-30, (f) MeOH-40, (g) MeOH-100 (methanol).

### Fourier Transform Infrared Spectroscopy

FTIR was carried out to investigate the short-range interactions between the solvents and the polymeric chains in the swollen membranes. Figure 1 shows the FTIR spectra of the unswollen and swollen Nafion membranes equilibrated after immersion in water, methanol, and water-methanol mixtures at 35°C. The characteristic IR bands associated with the functional groups of Nafion and the solvents are seen in the FTIR spectra, including<sup>34</sup>: the OH stretching ( $\nu \sim 3600\text{--}3000\text{ cm}^{-1}$ ) and bending ( $\nu \sim 1650\text{ cm}^{-1}$ ) vibrations; the Nafion C—F, C—C, and  $\text{SO}_3^-$  ( $\nu \sim 1400\text{--}1050\text{ cm}^{-1}$ ) and C—O—C stretching ( $\nu \sim 1040\text{--}940\text{ cm}^{-1}$ ) bands. As expected, an increase in the intensity of the OH vibration regions of the spectrum of the membranes is observed after swelling, due to the absorption of solvent. The spectra **c** to **g** in Figure 1 also show peaks at  $1060\text{ cm}^{-1}$  (C—O st. vibration),  $2945\text{ cm}^{-1}$  and  $2833\text{ cm}^{-1}$  (C—H stretching vibrations) associated with absorbed methanol.<sup>35</sup>

The assignment of the bands corresponding to the different OH vibration modes are listed in Table II. The broad dispersion of

the OH stretching band at  $\nu < 3000\text{ cm}^{-1}$  extending to the bending regions  $\nu > 1650\text{ cm}^{-1}$  indicates IR continuum absorption and was interpreted by Zundel as originating from the delocalization of the proton vibration by the formation of solvent clusters ( $\text{H}_3\text{O}^+$ ,  $\text{CH}_3\text{OH}_2^+$ ...).<sup>42</sup> This phenomenon is typical for IR spectra of aqueous acidic media and has been extensively reported in the literature with regard to Nafion hydration.<sup>34,38–40,42</sup> The presence of the protonated species is consistent with the observation of the  $\text{SO}_3^-$  stretching band ( $\nu \sim 1060\text{ cm}^{-1}$ ) arising from the dissociation of the  $\text{SO}_2\text{OH}$  groups.<sup>34,38</sup>

Several changes are visible in the OH stretching region of the IR spectra of the Nafion membranes after solvent absorption. To study this region in detail, since several contributions are expected in this region of the spectrum (see Table III), the  $3600 < \nu < 2000\text{ cm}^{-1}$  frequency range of the FTIR spectra has been fitted using a sum of two Gaussian curves and an asymmetric curve; the latter was used to fit the high dispersion contribution at lower wavenumbers. The mathematical expression used for this fitting procedure is:

$$y = \sum_{i=1}^2 A_i \cdot \exp\left(-0.5 \cdot \frac{(x - x_{ci})^2}{w_i^2}\right) + A_3 \cdot \left(\frac{1}{1 + \exp\left(\frac{-(x - x_{c3} + 0.5)}{w_{23}}\right)}\right) + \left(1 - \frac{1}{1 + \exp\left(\frac{-(x - x_{c3} - 0.5)}{w_{33}}\right)}\right)$$

where  $A_i$  represents the intensity of the curve;  $x_{ci}$  is the frequency of the maximum absorbance;  $w_i$  describes the width of the Gaussian curve; and  $w_{23}$  and  $w_{33}$  the dispersion and shape of the asymmetric curve, respectively, and  $i$  is the number of curves used. An example of a deconvoluted spectrum is shown in Figure 2. The asymmetric peak (region  $\nu < 3000\text{ cm}^{-1}$ ) is attributed to the dispersion of the contribution of protonated species in the Nafion membranes, and may obscure the contributions of the C—H stretching modes of the methanol

**Table II.** Assignments of the OH Vibration Bands Seen in the Spectra Shown in Figure 1

Region ( $\text{cm}^{-1}$ )	Subregion ( $\text{cm}^{-1}$ )	Assignment	References
3800–2400 OH Stretching	3800–3600	OH forming weak H-bonds between the solvent molecules and the hydrophobic regions of Nafion through the hydrophobic-hydrophilic interface	36, 37
	3600–3400	OH groups of solvent molecules forming strong H-bonds with the polar groups of the polymer OH groups of solvent molecules interacting with ether groups	36, 37,38–41
	3400–3000	Bulk-like water and methanol molecules. Solvation and external OH groups in the solvent clusters	42
	3000–	$\text{H}_3\text{O}^+$ , $\text{H}_5\text{O}_2^+$ , $\text{CH}_3\text{OH}_2^+$ grouping species forming clusters in the membranes by dissociation of $\text{SO}_2\text{OH}^*$ Internal OH groups in the solvent clusters	38, 39, 42
2000–1400 OH bending	$\sim 1688$	Structural vibrations of Nafion	
	$\sim 1630$	External OH in solvent clusters	35, 42

**Table III.** Parameters of the Curves Used to Fit the OH Stretching Region of the FTIR Spectra of the Membranes

Sample	Region 3500 cm <sup>-1</sup>			Region 3300 cm <sup>-1</sup>			Region 3000 cm <sup>-1</sup>		
	Peak (cm <sup>-1</sup> )	Area (%·cm <sup>-1</sup> )	Width (cm <sup>-1</sup> )	Peak (cm <sup>-1</sup> )	Area (%·cm <sup>-1</sup> )	Width (cm <sup>-1</sup> )	Peak (cm <sup>-1</sup> )	Area (%·cm <sup>-1</sup> )	Width (cm <sup>-1</sup> )
Unswollen Nafion	3502	23.5	241	3340	11.9	297	3107	71.6	935
MeOH-0	3479	29.4	264	3278	11.2	251	3066	60.9	914
MeOH-10	3500	28.8	278	3253	37.6	422	2872	21.9	540
MeOH-20	3508	44.5	262	3280	56.8	401	2879	32.1	640
MeOH-30	3504	59.9	253	3298	85.6	372	2926	30.2	530
MeOH-40	3502	65.5	255	3296	92.9	372	2922	29.9	536
MeOH-100	3496	50.2	251	3286	82.6	392	2922	31.4	497

molecules.<sup>36,41,43</sup> The two peaks at  $\nu \sim 3500$  cm<sup>-1</sup> and  $\nu \sim 3300$  cm<sup>-1</sup> are assigned to solvent less affected by the presence of protonated species, involved in stronger ( $\nu \sim 3300$  cm<sup>-1</sup>) and weaker ( $\nu \sim 3500$  cm<sup>-1</sup>) interactions. We must take into account that the band at  $\nu \sim 3300$  cm<sup>-1</sup> may be obscured by an overtone of the OH bending vibration at  $\nu \sim 1630$  cm<sup>-1</sup> ( $2 \cdot \nu$ ).<sup>37,39</sup>

The changes observed in the OH stretching region of the FTIR spectra were quantified by calculating the position ( $\nu_i$ ), area ( $A_i$ ), maximum height ( $Abs_i$ ) and width at half of the maximum absorbance ( $\Delta\nu_i$ ) of the three individual peaks (listed in Table III). The intensities of the fitting peaks at higher wavenumbers ( $\nu \sim 3500$  cm<sup>-1</sup> and  $\nu \sim 3300$  cm<sup>-1</sup>) increase in the swollen membranes, this effect being more pronounced for the membranes immersed in solutions richer in methanol ( $C_{MeOH} > 20\%$ , wt %). An opposite effect is observed for the asymmetric peak (region  $\nu < 3000$  cm<sup>-1</sup>), which suggests that the formation of protonated species in Nafion is reduced by the presence of methanol.<sup>39</sup>

The individual dependence of each band on the composition was studied (Figure 3) and the ratios of their individual areas ( $A_{3300}/A_{3500}$ ) and maximum heights ( $Abs_{3300}/Abs_{3500}$ ) were calculated and are shown in Figure 4. On increasing methanol concentration, the peak at 3330 cm<sup>-1</sup> increases in intensity rela-

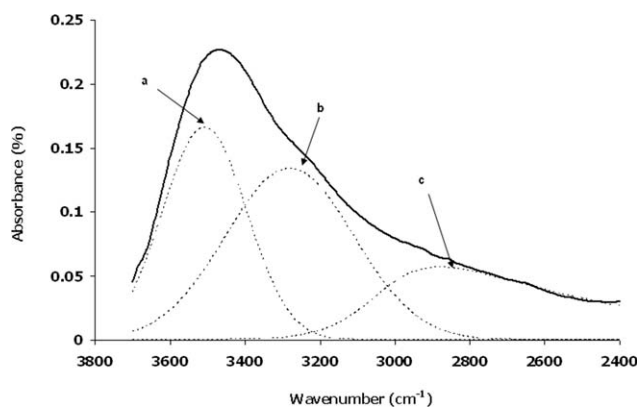


**Figure 2.** Deconvolution of the  $3700 < \nu < 2400$  cm<sup>-1</sup> region of the FTIR spectrum of a swollen Nafion membrane (MeOH-20): (a)  $\nu \sim 3500$  cm<sup>-1</sup>, (b)  $\nu \sim 3300$  cm<sup>-1</sup> (c)  $\nu < 3000$  cm<sup>-1</sup> ( $R^2 = 0.9997$ ).

tive to the peak at 3500 cm<sup>-1</sup>, and this coincides with a concurrent growth of the OH bending regions at lower wavenumbers ( $\nu \sim 1630$  cm<sup>-1</sup>). This suggests that methanol can be found in different molecular environments than water in the swollen Nafion membranes.

Some changes are also visible in the position of the individual  $\nu \sim 3500$  cm<sup>-1</sup> and  $\nu \sim 3300$  cm<sup>-1</sup> bands depending on the swelling mixture (Table III):

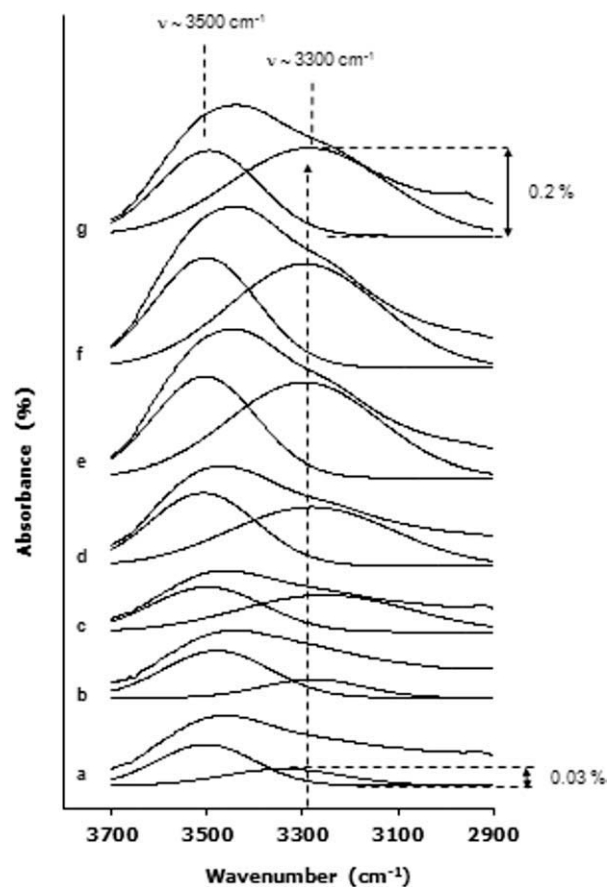


**Figure 3.** The deconvoluted region of the FTIR spectra of the Nafion membranes showing the peaks at 3300 cm<sup>-1</sup> and 3500 cm<sup>-1</sup>. (a) Unswollen Nafion, (b) MeOH-0, (c) MeOH-10, (d) MeOH-20, (e) MeOH-30, (f) MeOH-40, (g) MeOH-100.

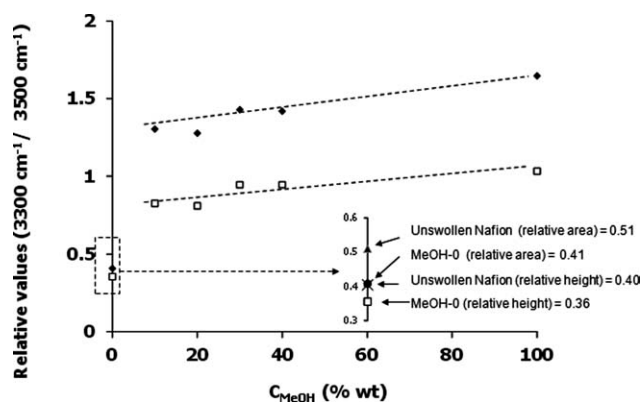


**Figure 4.** Relative values of area (*A*) and absorbance (*Abs*) of the peak at 3300 cm<sup>-1</sup> with respect to the peak at 3500 cm<sup>-1</sup> (deconvolution results). (◆) relative area (*A*<sub>3300</sub>/*A*<sub>3500</sub>) and (□) relative absorbance (*Abs*<sub>3300</sub>/*Abs*<sub>3500</sub>).

- The band in the 3500 cm<sup>-1</sup> region appears at higher wavenumbers for membranes swollen in the mixtures than in either pure water ( $\nu = 3418$  cm<sup>-1</sup>) or methanol ( $\nu = 3349$  cm<sup>-1</sup>). This is consistent with the results found by Falk and Buzzoni, and indicates the formation of weaker hydrogen bonds by the solvents absorbed in Nafion.<sup>36,37,39</sup>
- Shifts are observed in this peak with respect to the unswollen membrane ( $\nu = 3502$  cm<sup>-1</sup>). Specifically, the position of the band is located at  $\nu = 3479$  cm<sup>-1</sup> for MeOH-0 and at  $\nu = 3496$  cm<sup>-1</sup> for MeOH-100. This suggests that the hydrogen bonds formed by the OH groups contributing to this band (possibly those in the solvation shell of the clusters) are sensitive to the presence of methanol.
- In contrast, a remarkable shift to lower frequencies of the  $\nu \sim 3300$  cm<sup>-1</sup> peak is observed in the FTIR spectra of the swollen membranes. We could assign this contribution to methanol molecules forming interactions with intermediate strengths between those responsible for the  $\nu \sim 3500$  cm<sup>-1</sup> band and those related to protonated complexes ( $\nu < 3000$  cm<sup>-1</sup>).

We will now consider the different regions of the FTIR spectra dominated by peaks associated with the functional groups of Nafion. First, the FTIR spectra of all the samples in the 1400–1000 cm<sup>-1</sup> region have been fitted to a sum of six Gaussian contributions, corresponding to the characteristic IR absorption bands assigned for Nafion (see Table IV).<sup>34,38</sup> The corresponding fitting parameters of each peak (position,  $\nu_i$ , area, *A<sub>i</sub>*, and width,  $\Delta\nu_i$ ) were calculated with high *R*<sup>2</sup> ( $\sim 0.9990$ ). Figure 5 shows the case for the unswollen Nafion membrane along with the six corre-

**Table IV.** Assignments of the FTIR Vibration Bands Associated with Nafion

Assignment	$\nu_{\max}$ (cm <sup>-1</sup> )	Assignment	$\nu_{\max}$ (cm <sup>-1</sup> )	Assignment	$\nu_{\max}$ (cm <sup>-1</sup> )
$\nu_{\text{as}}(\text{CF}_2)$	1240	$\nu_{\text{as}} \text{SO}_3^-$	1130	$\delta(\text{CF}_2)$	525
	1153	$\nu_s \text{SO}_3^-$	1057	$\tau(\text{CF}_2)$	558
$\nu_{\text{as}}(\text{C}-\text{C})$	1317	$\nu_s \text{COC}$	940–1010	$\omega(\text{CF}_2)$	636
	1294			$\nu_s(\text{CF}_2)$	718
				$\nu(\text{C}-\text{S})$	805

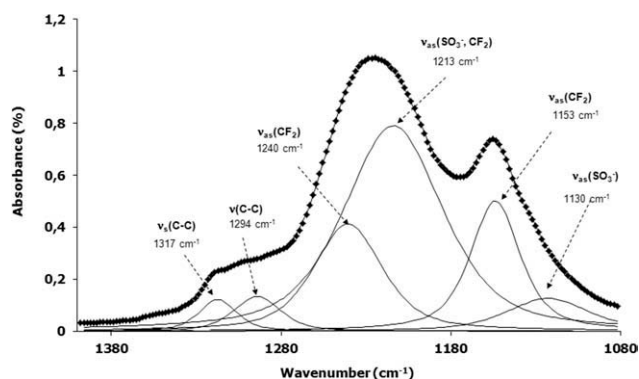


**Figure 5.** Deconvolution of the 1000–1400 cm<sup>-1</sup> region of the FTIR spectrum of unswollen Nafion. ◆ corresponds to the experimental points, solid line to the fitted curve and dotted lines to the individual Gaussian contributions.

sponding fitting peaks. Solvent absorption results in changes in this IR region, and the values of the four fitting peaks corresponding to characteristic bands of the perfluorinated regions and sulfonate groups are listed in Table V. The results corresponding to the 1057 cm<sup>-1</sup> band ( $\nu_s(\text{SO}_3^-)$ ) were obtained separately by using a similar fitting procedure and are also listed in Table V.

The FTIR bands associated with the  $\text{SO}_3^-$  and  $\text{CF}_2$  groups show different dependencies on the solvent composition. The area of the peaks related to the sulfonate groups tends to increase when the membrane is swollen in water, but decrease on increasing the methanol concentration in the mixtures, and an opposite trend is observed for regions related to the perfluorinated matrix ( $\text{CF}_2$ ). Similar results reported for dehydration studies of Nafion were interpreted as modification in the interactions involving the polymer groups due to the variation of protonated species (highly functional polar) and the number of acid-basic species.<sup>34,39</sup> This view is consistent with the reduction in intensity of the continuous OH stretching band ( $\nu < 3000$  cm<sup>-1</sup>) described earlier.<sup>38,39,44</sup> Our data suggest, therefore, that methanol promotes weaker interactions with the sulfonate groups and a simultaneous increase on the perturbation of the hydrophobic regions of Nafion.

It is clear, therefore, that the solvent absorbed effects the environment of the different groups of Nafion. Halliman and Elab attributed the differences in the transport profiles observed for methanol and water mixtures in Nafion to variations of the free volume in the hydrophilic phase.<sup>35</sup> However, there is not a completely satisfying explanation for methanol absorption in Nafion.<sup>1</sup> One of the most controversial points is the role of the side chains and the existence of amorphous hydrophilic regions which may participate in the absorption of polar solvents.<sup>27</sup> IR studies have revealed the existence of specific interactions between the solvents and the C—O—C groups of the PFAE side chains of swollen Nafion.<sup>38,43,45,46</sup> In an attempt to investigate similar effects in our samples, we studied the symmetric C—O—C stretching vibration region ( $\nu \sim 1010$ – $940$  cm<sup>-1</sup>) of the spectrum with greater detail, following similar methodology as in the previous regions. The experimental spectra were fitted to three bands located at  $\nu_1 \sim 970$  cm<sup>-1</sup>,  $\nu_2 \sim 983$  cm<sup>-1</sup>, and  $\nu_3 \sim 993$  cm<sup>-1</sup>, as shown in Figure 6. The normalised areas of

**Table V.** Parameters of the Curves Used to Fit the OH Stretching Region of the FTIR Spectra of the Nafion Membranes

Sample	SO <sub>3</sub> <sup>-</sup> st				CF <sub>2</sub> st			
	$v_{\max}$ (cm <sup>-1</sup> )	Area cm <sup>-1</sup> (%)	$v_{\max}$ cm <sup>-1</sup>	Area cm <sup>-1</sup> (%)	$v_{\max}$ cm <sup>-1</sup>	Area cm <sup>-1</sup> .%	$v_{\max}$ cm <sup>-1</sup>	Area cm <sup>-1</sup> .%
Unswollen Nafion	1122	8.2	1057	2.2	1240	25.0	1153	22.6
MeOH-0	1126	10.4	1057	2.0	1238	21.4	1153	16.2
MeOH-10	1128	10.3	1057	1.9	1238	22.7	1153	15.1
MeOH-20	1134	10.0	1057	2.0	1240	26.7	1155	18.3
MeOH-30	1136	8.3	1057	1.6	1240	29.7	1157	17.1
MeOH-40	1132	4.8	1057	1.6	1238	41.1	1155	19.8
MeOH-100	1132	5.7	1057	1.2	1238	38.2	1157	19.1

the individual peaks ( $A_i$ ) calculated by simple integration are listed in Table VI. The fitting peaks at lower wavenumbers ( $v_1 \sim 970$  cm<sup>-1</sup> and  $v_2 \sim 983$  cm<sup>-1</sup>) tend to decrease in intensity at higher methanol concentrations, while the converse is true for the peak at higher wavenumbers ( $v_3 \sim 993$  cm<sup>-1</sup>).

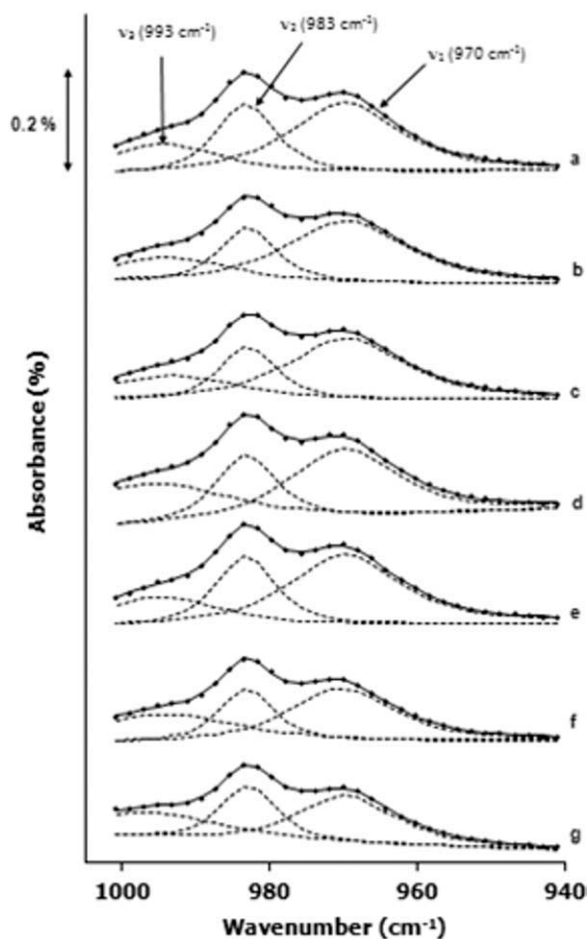


**Figure 6.** The ether (COC) vibration region (940–1100 cm<sup>-1</sup>) of the FTIR spectra: (a) Unswollen Nafion, (b) MeOH-0, (c) MeOH-10, (d) MeOH-20, (e) MeOH-30, (f) MeOH-40, (g) MeOH-100. ♦ corresponds to the experimental points, solid line to the fitted curve and dotted lines to the individual Gaussian contributions.

These solvent-composition dependent changes suggest that the ether groups of the side chains of Nafion are also somehow involved in the absorption of the solvents.<sup>39</sup> Although there is no clear consensus concerning the assignments of the peaks in the ether region of the FTIR spectrum,<sup>1</sup> Cable and Falk associated the bands at higher wavenumbers to structural vibrations of ether bonds, which were already present in the nonionic PTFE-based predecessor of Nafion, and the bands at lower frequencies to groups more affected by the sulfonate groups, and probably related to the formation of ionic clusters.<sup>45,47</sup> According to these assignments, the observed increase in the intensity of the band at  $v_3 \sim 993$  cm<sup>-1</sup> at higher methanol concentrations may be interpreted as an increase of the interactions between solvent molecules and C—O—C groups more shielded from the clusters, i.e., more related to the nonpolar phase (see Figure 7).

#### Thermogravimetric Analysis

Figure 8 shows the first derivative thermogravimetric (DTG) curves of the Nafion membranes before and after the absorption tests were performed. The decomposition of unswollen Nafion (trace a) occurs following a complex degradation process involving several steps. First, at lower temperatures (25–250°C), we see a number of weak peaks which may be attributed to the volatilization of solvents, presumably mainly water, from the membrane ( $\Delta w = 5.70\%$ ). The existence of several peaks in the 100–250°C region suggests that a fraction of the solvent may be

**Table VI.** Parameters Associated with the Peaks Used to Fit the COC Region (940–1010 cm<sup>-1</sup>) of the FTIR Spectra

Sample	Fractional area contribution (COC region)		
	$v_3$ (993 cm <sup>-1</sup> )	$v_2$ (983 cm <sup>-1</sup> )	$v_1$ (970 cm <sup>-1</sup> )
Unswollen Nafion	0.12	0.34	0.54
MeOH-0	0.12	0.30	0.58
MeOH-10	0.11	0.30	0.58
MeOH-20	0.13	0.33	0.55
MeOH-30	0.21	0.30	0.49
MeOH-40	0.26	0.27	0.47
MeOH-100	0.33	0.27	0.40

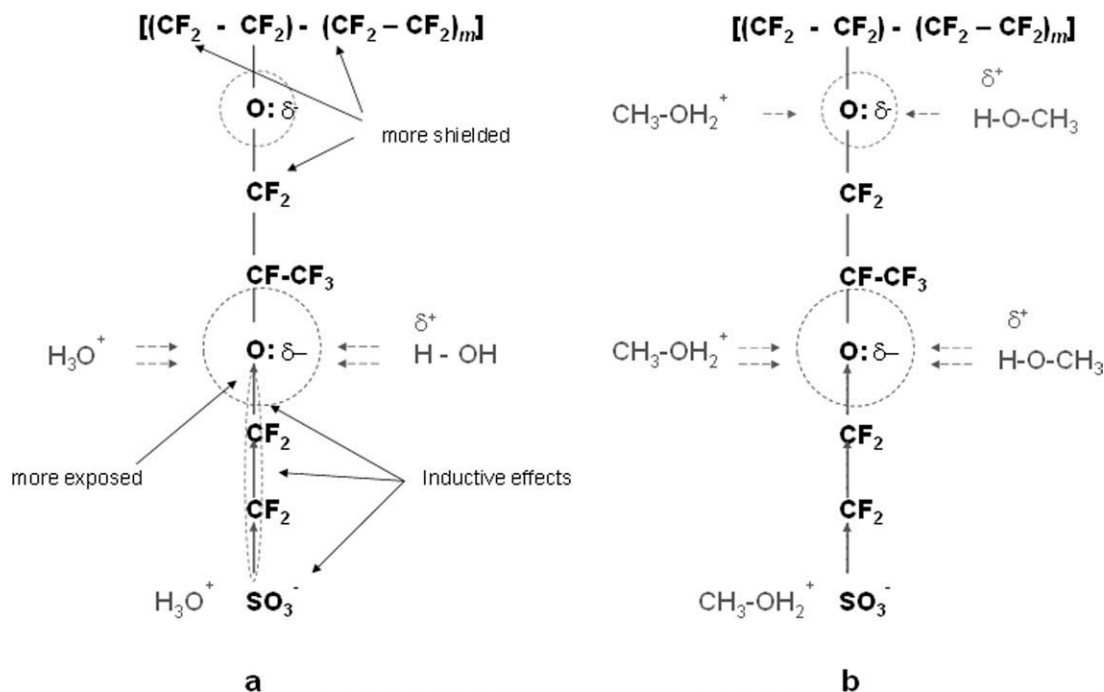


Figure 7. Schematic representation of the formation of complexes between the ether groups and solvents: (a) water, (b) methanol.

tightly bound to the polymer structure.<sup>45,47</sup> The degradation of Nafion starts at  $T > 250^{\circ}\text{C}$ , probably by desulfonation in the  $250\text{--}390^{\circ}\text{C}$  region (maximum mass loss rate at  $T_p = 348^{\circ}\text{C}$ ).<sup>48,49</sup> Several weak peaks are observed between  $390$  and  $470^{\circ}\text{C}$ , with a maximum at  $T_p = 457^{\circ}\text{C}$ , which have been attributed to the degradation of the side chains of the polymer.<sup>47–50</sup> Finally, at high temperatures, two strong peaks are seen, associated with the decomposition of the PTFE backbone ( $T_p = 475^{\circ}\text{C}$  and  $T_p = 501^{\circ}\text{C}$ ).<sup>51</sup> The residual fraction of Nafion at  $750^{\circ}\text{C}$  was 0.63% of the initial mass. These observations are consistent with those reported in the literature.<sup>47,52,53</sup>

A number of differences are seen in the DTG curves of the swollen membranes when compared to that of the unswollen Nafion sample. First, in the  $100\text{--}250^{\circ}\text{C}$  region (Figure 9) an increase in intensity of the curves for higher methanol concentrations is observed, consistent with the increase of solvent absorption reported in the swelling tests and FTIR sections. However, the peaks in the  $100\text{--}250^{\circ}\text{C}$  region increase more markedly than those below  $100^{\circ}\text{C}$  (solvent already present in the starting Nafion and loosely absorbed). This suggests that the absorption of solvent tightly bound to the polymer is promoted by the presence of methanol.<sup>27,47</sup>

The absorption of solvent also affects the thermal degradation of Nafion (region  $250\text{--}650^{\circ}\text{C}$ ). To study this region in more detail, and due to the presence of several overlapping processes, the DTG curves were fit by five Gaussian peaks. An example of the deconvolution of this temperature region of the DTG curve for the membrane immersed in pure water (MeOH-0) is shown in Figure 10. The use of five peaks gave a satisfactory fitting ( $R^2 > 0.9990$ ). The parameters corresponding to the individual peaks were calculated, and the area ( $A_i$ , wt %) and temperature at the maximum intensity ( $T_{pi}$ ) are listed in Table VII. Solvent

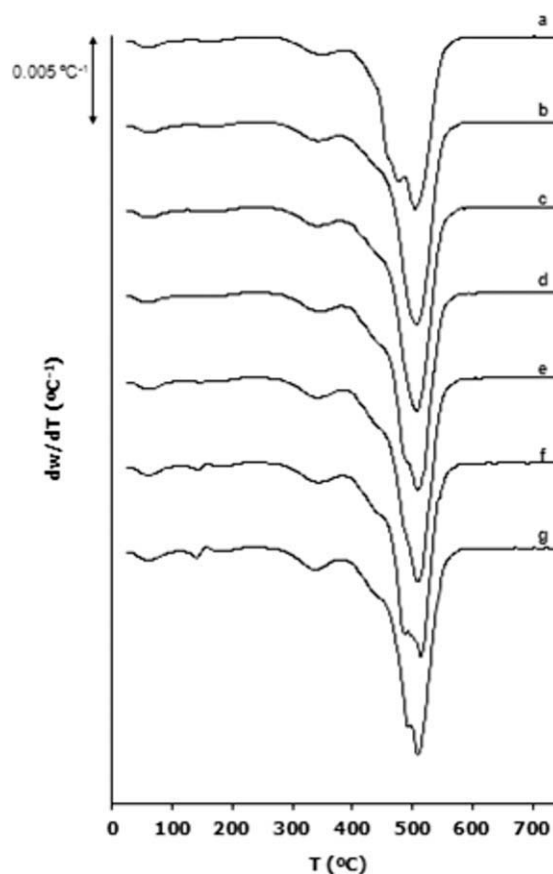
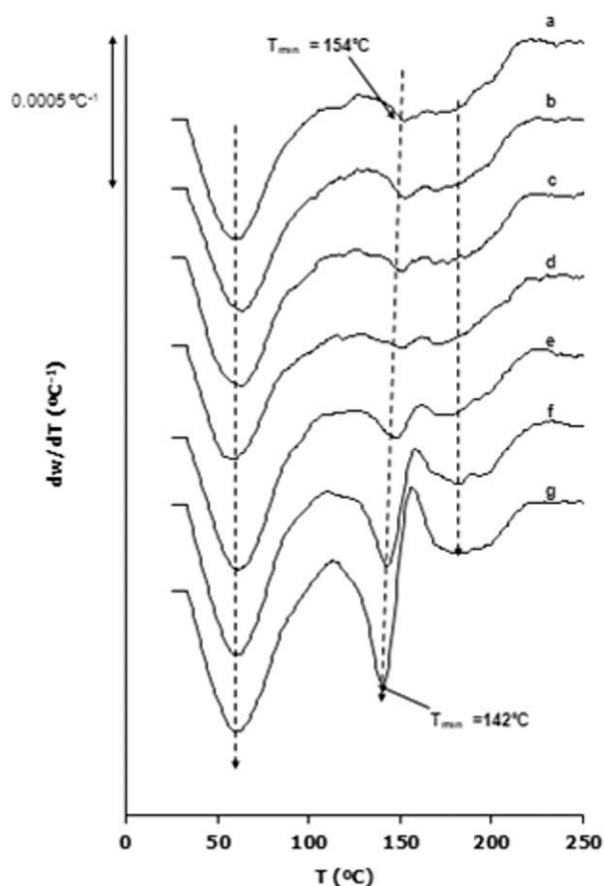
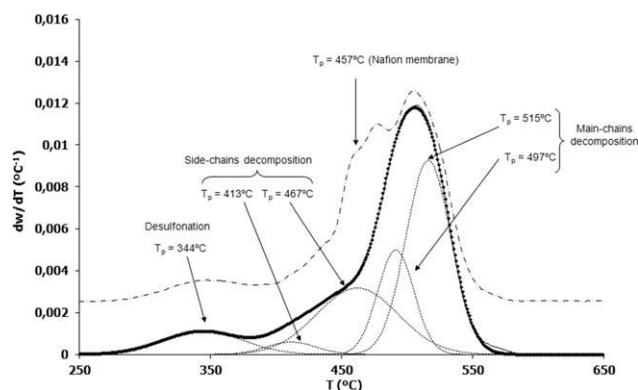


Figure 8. DTG curves of the Nafion membranes immersed in water and methanol mixtures at  $35^{\circ}\text{C}$ : (a) Unswollen Nafion, (b) MeOH-0 (water) (c) MeOH-10, (d) MeOH-20, (e) MeOH-30, (f) MeOH-40, (g) MeOH-100 (methanol).



**Figure 9.** DTG curves of the Nafion membranes immersed in water and methanol mixtures at 35°C. Low temperatures region ( $T < 250^{\circ}\text{C}$ ): (a) Unswollen Nafion, (b) MeOH-0, (c) MeOH-10, (d) MeOH-20, (e) MeOH-30, (f) MeOH-40, (g) MeOH-100.

absorption appears to shift the desulfonation process (250–400°C) to lower temperatures, with the maximum reduction occurring for the sample swollen in pure methanol (MeOH-100). This may be explained by a decrease in the interactions between the sulfonate groups in the swollen Nafion membranes, which is most pronounced at higher methanol concentrations.



**Figure 10.** Deconvolution of the DTG curve for the Nafion membranes in the 250–650°C region. The solid line corresponds to the membrane absorbed in water (MeOH-0) and the dotted line (-----) to unswollen membrane. The individual Gaussian contributions are also plotted (—).

Solvent absorption also seems to promote some slight changes in the shape of the DTG curves regarding the thermal degradation of Nafion, especially in samples absorbing methanol, although no dramatic changes are observed in the maximum of the peaks. These results can be attributed to reorganization of the material (see Figure 10) and reinforce the view that methanol absorption affects the polymeric matrix of Nafion to a greater extent than water.

### Differential Scanning Calorimetry

DSC was used as an attempt to describe some of the morphology changes in Nafion caused by the solvent absorption. The thermograms obtained on the first heating scan of the Nafion membranes showed a broad, strong endothermic peak appears between 20 and 120°C. Because the main peak is not observed in the subsequent cooling or second heating scans, it was assigned to the loss of water or other solvents from the membranes.<sup>48</sup> The values of the enthalpy change,  $\Delta H_1$  ( $\text{J g}^{-1}$ ), and peak temperature,  $T_1$  ( $^{\circ}\text{C}$ ), obtained for all the samples are listed in Table VIII, and as expected, there is an increase in  $\Delta H_1$  for the swollen membranes. Neither  $\Delta H_1$  nor  $T_1$  show a simple dependency on solvent composition.

**Table VII.** Parameters of the Peaks Used to Deconvolute the 250–650°C Region of the DTG Curves Obtained for the Nafion Membranes

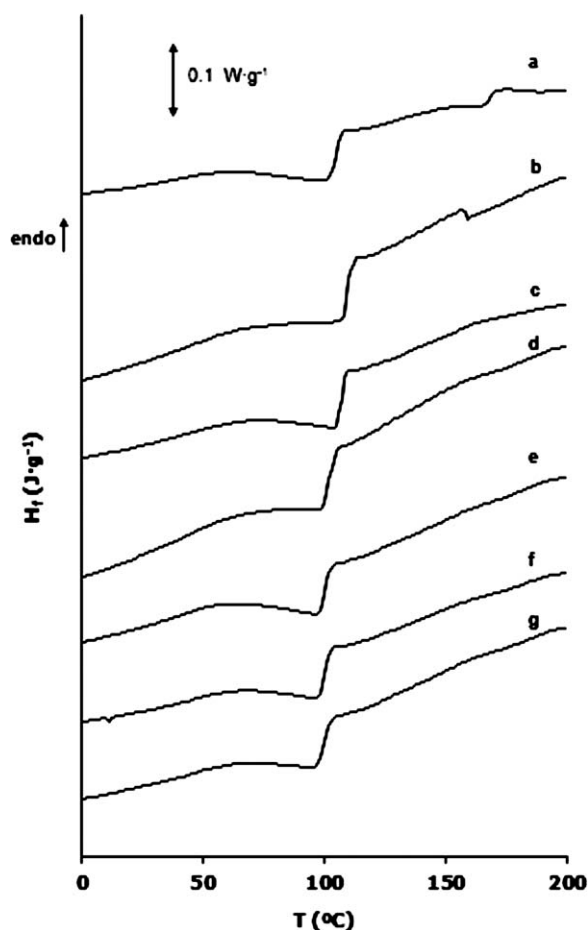
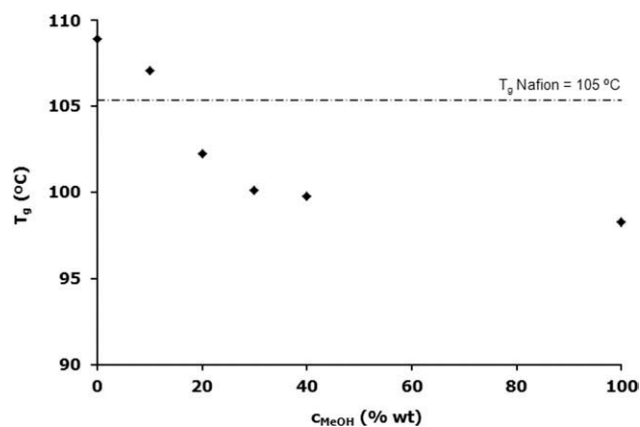
Sample	Residual (%)	Desulfonation process		Side-chains decomposition (low temperatures)		Main-chains decomposition (low temperatures)		Main-chains decomposition (high temperatures)	
		$T_{pi}$ ( $T_i$ , °C)	Area ( $A_i$ , %)	$T_{pi}$ (°C)	$A_i$ (%)	$T_{pi}$ (°C)	$A_i$ (%)	$T_{pi}$ (°C)	$A_i$ (%)
Unswollen Nafion	0.6	348	8.2	457	3.2	473	7.1	511	38.4
MeOH-0	0.5	344	8.5	413	2.8	497	20.1	515	54.3
MeOH-10	0.6	343	8.3	412	3.0	497	19.4	515	54.1
MeOH-20	0.5	346	8.7	427	2.6	484	10.6	512	62.8
MeOH-30	1.0	344	9.0	423	4.6	482	13.5	511	63.5
MeOH-40	1.5	341	7.6	420	5.1	485	21.7	512	58.6
MeOH-100	1.2	340	8.0	–	–	488	17.1	511	62.6



**Table VIII.** Thermal Data Extracted from the DSC Scans of the Nafion Membranes

Sample	$T_1$ (°C)	$\Delta H_1$ (J g <sup>-1</sup> )	$T_g$ (°C)	$\Delta C_p$ (J g <sup>-1</sup> K <sup>-1</sup> )·10 <sup>2</sup>
Unswollen Nafion	73	29.9	105	7.06
MeOH-0	77	76.9	109	9.32
MeOH-10	80	79.6	107	8.18
MeOH-20	73	72.8	102	8.26
MeOH-30	75	75.3	100	7.06
MeOH-40	74	73.9	100	6.92
MeOH-100	75	75.3	98	6.26

Because the desorption endotherm overlapped other thermal transitions visible in the  $-50$  to  $200^\circ\text{C}$  temperature region, the DSC thermograms on their reheating scans were obtained, and are shown in Figure 11. All the samples exhibit similar traces to that seen for the unswollen Nafion (trace a). A thermal transition is visible at about  $100^\circ\text{C}$  which can be attributed to a glass transition of the polar phase of Nafion.<sup>47,52,54</sup> The appearance of this transition in all the samples indicates that the Nafion membranes retain their cluster morphology after being submit-

**Figure 11.** DSC traces for the Nafion membranes used in the swelling tests. Second heating scan: (a) Unswollen Nafion, (b) MeOH-0, (c) MeOH-10, (d) MeOH-20 (e) MeOH-30, (f) MeOH-40, (g) MeOH-100.**Figure 12.** Values of  $T_g$  obtained from the DSC second heating scans of the unswollen and swollen Nafion membranes.

ted to the swelling tests. The glass transition temperature ( $T_g$ ) and the change in the specific heat capacity ( $\Delta C_p$ ) of this transition are also listed in Table VIII. The dependence of  $T_g$  on the concentration of methanol in the swelling experiments is shown in Figure 12. The MeOH-0 and MeOH-10 membranes show higher  $T_g$  values than the unswollen Nafion, while at higher methanol concentrations, the glass transition falls below that of Nafion, reaching a limiting value corresponding to that of the membrane swollen in pure methanol (MeOH-100,  $T_g = 105^\circ\text{C}$ ).  $\Delta C_p$  also tends to decrease on increasing the concentration of methanol in the mixtures.

Nafion shows a phase separated morphology comprising polar and nonpolar regions, which may be described in terms of the size and distribution of the ionic clusters that minimize the interfacial force between these regions.<sup>25,52</sup> In the samples swollen with higher water contents (MeOH-0 and MeOH-10), the increase in  $T_g$  and  $\Delta C_p$  can be interpreted as an increase in the size of the ionic clusters in the Nafion membranes driven by water absorption. Such a coalescence process has been widely described in the literature.<sup>3</sup> Within this framework of spherical clusters connected by narrow channels proposed by Gierke and co-workers, the growth of clusters with increasing water content is proposed to occur by a combination of expansion in cluster size and a redistribution of the sulfonate sites to yield fewer clusters in the hydrated material.<sup>13,14</sup> The decreases in  $T_g$  and  $\Delta C_p$  at high methanol concentrations may indicate that the coalescence of ionic domains in those membranes may be inhibited, despite the higher amounts of solvent absorbed. These results reinforce the view that the morphology of the swollen membranes is controlled, to some extent, by the absorption of methanol and methanol/water mixtures. The differences in these morphologies may be accounted for either by the tendency for the solvent to be absorbed in the nonpolar phases (as described in the FTIR and TGA sections), or by plasticizing effects of the organic solvents on the side chains.<sup>20,55,56</sup>

## CONCLUSIONS

The combination of thermal analytical and spectroscopic techniques revealed changes in the interactions regarding water, methanol and water-methanol mixtures absorbed in commercial

Nafion membranes. These differences were attributed to a major influence of the nonpolar domains (hydrophobic regions) of Nafion in the absorption of methanol and a reduction of the interactions with sulfonate groups (hydrophilic regions). This results in an increase of tightly bound solvent in the membranes and changes in the polar phase morphology, probably by inhibiting the coalescence process of the ionic clusters. An improved understanding of these effects may be important to determine the resulting microstructure of Nafion and its behavior when used as electrolyte in the presence of polar solvents.

#### ACKNOWLEDGMENTS

The authors thank the financial support of the Generalitat Valenciana, through the Grisolia and Forteza programs, and the Spanish Ministry of Science and Innovation, through the Research Projects ENE2007-67584-C03, UPOV08-3E-013, IT2009-0074, ENE2011-28735-C02-01 and the awarding of two FPI and FPU predoctoral grants.

#### REFERENCES

- Mauritz, K. A.; Moore, R. B. *Chem. Rev.* **2004**, *104*, 4535.
- Blomen, L. *Fuel Cell Systems*; Plenum Press, New York, **1993**.
- Larminie, J.; Dicks, A. *Fuel Cell Systems Explained*, 2nd ed.; Wiley: New York, **2003**.
- Kerres, J. A. *J. Memb. Sci.* **2001**, *185*, 3.
- Elabd, Y. A.; Hickner, M. A. *Macromolecules* **2011**, *44*, 1.
- Grot, W. G. *Macromol. Symp.* **1994**, *82*, 161.
- DeLuca, N. W.; Elabd, Y. A. *J. Polym. Sci. Part B: Polym. Phys.* **2006**, *44*, 2201.
- Ravikumar, M. K.; Shukla, A. K. *J. Electrochem. Soc.* **1996**, *143*, 2601.
- Scott, K.; Taama, W.; Cruickshank, J. J. *Appl. Electrochem.* **1998**, *28*, 289.
- Ge, J.; Liu, H. J. *Power Sources* **2005**, *142*, 56.
- Elabd, Y. A.; Napadensky, E.; Sloan, J. M.; Crawford, D. M.; Walker, C. W. *J. Membr. Sci.* **2003**, *217*, 227.
- Yang, C. C.; Chiu, S. J.; Chien, W. C. *J. Power Sources* **2006**, *162*, 21.
- Hsu, W. Y.; Gierke, T. D. *J. Membr. Sci.* **1983**, *13*, 307.
- Gierke, T. D.; Munn, G. E.; Wilson, F. C. *J. Polym. Sci. Part B: Polym. Phys.* **1981**, *19*, 1687.
- Yeager, H. L.; Steck, A. J. *J. Electrochem. Soc.* **1981**, *128*, 1880.
- Fujimura, M.; Hashimoto, T.; Kawai, H. *Macromolecules* **1981**, *14*, 1309.
- Horkay, F.; Zrinyi, M. *Macromolecules* **1982**, *15*, 1306.
- Dreyfus, B.; Gebel, G.; Aldebert, P.; Pineri, M.; Escoubes, M. J. *Phys. (Paris)* **1990**, *51*, 1341.
- Litt, M. H. *Polym. Prepr.* **1997**, *38*, 80.
- Haubold, H. G.; Vad, T. H.; Jungbluth, H.; Hiller, P. *Electrochim. Acta* **2001**, *46*, 1559.
- Rubatat, L.; Rollet, A. L.; Gebel, G.; Diat, O. *Macromolecules* **2002**, *35*, 4050.
- Kumar, S.; Pineri, M. J. *Polym. Sci. Part B: Polym. Phys.* **1986**, *24*, 1767.
- Eisenberg, A. *Macromolecules* **1970**, *3*, 147.
- Mauritz, K. A.; Rogers, C. E. *Macromolecules* **1985**, *18*, 483.
- Gebel, G. *Polymer* **2000**, *41*, 5829.
- McLean, R. S.; Doyle, M.; Sauer, B. B. *Macromolecules* **2000**, *33*, 6541.
- Young, S. K.; Trevino, S. F.; Beck Tan, N. C. *J. Polym. Sci. Part B: Polym. Phys.* **2002**, *40*, 387.
- Wakisaka, A.; Abdoul-Carime, Y.; Yamamoto, Y.; Kiyozumi, Y. J. *Chem. Soc. Faraday Trans.* **1998**, *94*, 369.
- Urban, W. *Attenuated Total Reflectance Spectroscopy of Polymers, Theory and Practice*; American Chemical Society: Washington, DC, **1996**.
- Tury, A. *Thermal Characterization of Polymeric Materials*, Vol. 1; Academic Press: San Diego, **1997**.
- Venturi, M. T. *J. Mol. Struct.* **1972**, *14*, 293.
- Hietala, S.; Maunu, S. L.; Sundholm, F. J. *Polym. Sci. Part B: Polym. Phys.* **2000**, *38*, 3277.
- Saarinen, V.; Kreuer, K. D.; Schuster, M.; Merkle, R.; Maier, J. *Solid States Ionics* **2007**, *178*, 533.
- Gruger, A.; Régis, A.; Schmatko, T.; Colomban, P. *Vib. Spectrosc.* **2001**, *26*, 215.
- Hallinan, D. T., Jr.; Elabd, Y. A. *J. Phys. Chem. B* **2007**, *111*, 13221.
- Falk, M., *Can. J. Chem.* **1980**, *58*, 1495.
- Quezado, S.; Kwak, J. C. T.; Falk, M. *Can. J. Chem.* **1984**, *62*, 958.
- Ostrowska, J.; Narebska, A. *Colloid Polym. Sci.* **1983**, *261*, 93.
- Buzzoni, R.; Bordiga, S.; Ricchiardi, G.; Spoto, G.; Zecchina, A. *J. Phys. Chem.* **1995**, *99*, 11937.
- Zundel, G. *Easily Polarizable Hydrogen Bonds-Their Interaction with the Environment-IR Continuum and Anomalous Large Proton Conductivity*, in: *the Hydrogen Bond-Recent Developments in Theory and Experiments*, Vol. 2; Schuster, P.; Zundel, G.; Sandorfy, C., Eds.; North Holland: Amsterdam, **1976**; p 683.
- Mohr, S. C.; Wilk, W. D.; Barrow, G. M. *J. Am. Chem. Soc.* **1965**, *87*, 3048.
- Zundel, G. *The Hydrogen Bond* Schuster, P.; Zundel, G.; Sandorfy, C., Eds.; Amsterdam, **1979**, p 683.
- Heitner-Wirguin, C. *Polymer* **1979**, *20*, 371.
- Moynihan, R. E. *J. Am. Chem. Soc.* **1959**, *81*, 1045.
- Duplessix, R.; Escoubes, M.; Rodmacq, B.; Volino, F.; Roche, E.; Eisenberg, A.; Pineri, M. *Water in Polymers*, Rowlands ACS Symposium Series 127; ACS: Washington DC, **1980**; p 469.
- Eisenberg, A. *In perfluorinated Ionomer Membranes*; American Chemical Society: Washington DC, **1982**; p 139.

47. de Almeida, S. H.; Kawano, Y. J. *Therm. Anal. Calorim.* **1999**, *58*, 569.
48. Sun, L.; Thrasher, J. S. *Polym. Degrad. Stab.* **2005**, *89*, 43.
49. Shao, Z. G.; Joghee, P.; Hsing, I. M. *J. Membr. Sci.* **2004**, *229*, 43.
50. Wilkie, C. A.; Thomsen, J. R.; Mittleman, M. L. *J. Appl. Polym. Sci.* **1991**, *42*, 901.
51. Tiwari, S. K.; Nema, S. K.; Agarwal, Y. K. *Thermochim. Acta* **1998**, *317*, 175.
52. Stefanithis, I. D.; Mauritz, K. A. *Macromolecules* **1990**, *23*, 2397.
53. Feldheim, D. L.; Lawson, D. R.; Martin, C. R. *J. Polym. Sci. Part B: Polym. Phys.* **1993**, *31*, 953.
54. Yeo, S. C.; Eisenberg, A. J. *Appl. Polym. Sci.* **1997**, *21*, 875.
55. Meresi, G.; Wang, Y.; Bandis, A.; Inglefield, P. T.; Jones, A. A.; Wen, W.-Y. *Polymer* **2001**, *42*, 6153.
56. Gong, X.; Bandis, A.; Tao, A.; Meresi, G.; Inglefield, P. T.; Jones, A. A.; Wen, W.-Y. *Polymer* **2001**, *42*, 6485.